

TORSIONAL MODE DAMPING FOR ELECTRICALLY DRIVEN GAS COMPRESSION TRAINS IN EXTENDED VARIABLE SPEED OPERATION

by

Christof Sihler

Senior Research Engineer

Simon Schramm

Research Engineer

Joseph Song-Manguelle

Power Electronics Engineer

GE Global Research, Power Conversion Systems

Munich, Germany

Paola Rotondo

Senior Electrical Engineer

Stefano Del Puglia

Lead Electrical Engineer

GE Oil & Gas

Florence, Italy

and

Einar Larsen

Director

GE Energy Applications and System Engineering

Schenectady, New York

Christof Sihler is a Senior Research Engineer in the High Power Electronics Lab of GE Global Research Europe, in Munich, Germany. He joined GE in 2004 and, since then, has lead several R&D projects related to the system integration of large electrical drives.

Dr. Sihler received his Dipl.-Ing. and a Dr.-Ing. degree (Electrical Engineering) from the University of Karlsruhe. Before joining GE, he worked for three years at the Research Center Karlsruhe and for eight years as a Power Systems Engineer at the Max-Planck-Institute for Plasmaphysics in Garching, Germany.

Simon Schramm is a Research Engineer in the High Power Electronics Lab of GE Global Research (GEGR) Europe, in Munich, Germany. Since 2004 he has been involved with several R&D projects on power electronics and power systems at GEGR.

Mr. Schramm received his M.Sc. degree from the Munich University of Applied Sciences and is currently working on his Ph.D. degree thesis "Damping of Torsional Interaction Effects in Power Systems," at the Technische Universität München.

Joseph Song-Manguelle is a Power Electronics Engineer with the Electronic Power Conversion Lab of GE Global Research, in Niskayuna, New York. Since 2004, he has been involved in the design of high-power drives topologies and control for various applications. He was previously with Thermodyn, a GE oil and gas business in Le Creusot, France, as a Senior Electrical Engineer and team leader, dealing with torsional issues in compressor drive trains, including integrated high-speed motocompressor systems and testing high-power drives.

Dr. Song-Manguelle received a Ph.D. degree from the Swiss Federal Institute of Technology, Lausanne, Switzerland (2004), and an M.Sc. degree from the University of Douala, Cameroon (1997), both in Electrical Engineering.

Paola Rotondo is currently a Senior Electrical Engineer and Variable Speed Drives Systems Team Leader in the Electrical Department of GE Oil & Gas, in Florence, Italy. She joined GE in 2005 and is involved in requisition activities, string test support, and system simulations for several projects. Before joining GE, she was a researcher at Centro Laser, Valenzano, Italy, where she worked on the development of numerical and experimental medical and industrial models by using rapid prototyping techniques.

Ms. Rotondo received M.Sc. and Ph.D. degrees (Electrical Engineering) from Politecnico di Bari, Bari, Italy, in 2003 and 2007, respectively.

Stefano Del Puglia is a Lead Electrical Engineer in the Electrical Department of GE Oil & Gas in Florence, Italy. He joined GE in 2005, and, since then, has been involved in several projects with compressor trains driven by electric motors and LNG trains.

Dr. Del Puglia received his Dr.-Ing. degree (Electrical Engineering) from the University of Florence. Before joining GE, he worked for five years as an Electrical Design Engineer for power electronics and motor inverter design in Florence, Italy.

Einar Larsen is a Director with GE Energy Applications and System Engineering, in Schenectady, New York, where he has worked since graduation in 1974. His experience is in system engineering for applying new equipment to power grids. He is a Fellow of IEEE and the recipient of two major IEEE awards.

ABSTRACT

The oil and gas industry has a growing demand for electrically driven trains operated at variable speeds. Variable frequency electrical drives enable increased operational flexibility and energy efficiency. This is of great importance in applications requiring high power, such as gas compression.

Load commutated inverters (LCIs) are one of the most widespread technologies for driving large gas compression trains because of excellent reliability records. One drawback of power electronics driven systems is the generation of nonfundamental air-gap torque ripple components due to electrical harmonics. The air-gap torque ripple can interact with the mechanical system at torsional natural frequencies of the drive train.

Torsional vibration is an oscillatory angular motion that causes alternating twisting in shaft sections and machinery couplings. A consequence of uncontrolled excited torsional vibration may be a protective trip of the motor, to prevent mechanical damage, such as a failed coupling or a broken shaft.

This paper discusses illustrative design details of applying a torsional mode damping control system to LCI driven multi-Megawatt centrifugal gas compressors. The coincidence of electrical drive harmonics and torsional natural frequencies of the mechanical system is sometimes unavoidable due to the large variable speed range of the compressor such as for process requirements. For these types of applications, a power electronic damping system technology can be applied to new units or as a retrofit solution to existing variable speed trains.

The so-called integrated torsional mode damping (ITMD) unit is based on a torsional vibration measurement in the mechanical system and an interface to the existing inverter control of the drive system. The dc-link inductor of the LCI is partially used as an integrated energy storage unit and is combined with a smart damping controller, which reacts to a torsional vibration by modulating a small amount of the stored energy and sending it to the motor without impacting the normal operation of the system. As a result, the active power modulation at a torsional natural frequency of the mechanical system has a strong damping effect for torsional vibrations.

Intensive simulations and several tests were performed on large LCIs (up to 50 MW) over the last three years. Selected experimental results will be presented and discussed to validate the suggested damping system.

INTRODUCTION

There is an increasing trend in the oil and gas industry toward electrical drives rated for tens of Megawatts and rotational speeds around 3000 rpm, especially in high-power compressor trains as for example the liquefied natural gas (LNG) applications. A present role of these drives is as helpers and/or starters for the prime movers of compressor trains. Nowadays, such prime movers are typically gas turbines, but in some applications they are replaced/integrated by variable frequency drives, as reported by Baccani, et al. (2007).

Typical drive train configurations in oil and gas applications, such as LNG compression, are shown in Figure 1a-c. In configuration (a) the gas turbine (GT) drives the compressors and the electrical motor can act as a helper and/or starter. Another configuration of the compressor drive train is shown in Figure 1b. The electrical machine can operate as a GT starter or helper. The GT is used to drive the electrical machine and to generate electrical energy. In

this case, the machine operates as a generator. Using a power electronic converter enables the system to operate as a variable speed drive system. A fully electrical configuration is shown in Figure 1c. Redundant generators are typically used to increase the power system availability.

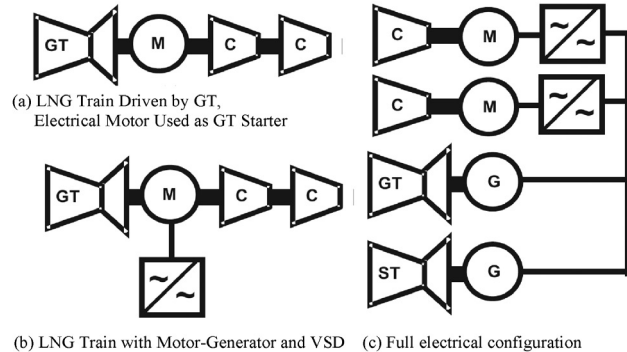


Figure 1. Typical Drive Train Configurations in Oil and Gas Applications.

In the oil and gas industry, the reliability of production processes is extremely important for the profitability of the investment. Drive manufacturers offer a large variety of converter topologies for variable speed drives (VSDs) in the Megawatt power range. For compressor applications in this nominal power range, there are basically two types of inverters that can be applied: A current source inverter, known as a load-commutated-inverter (LCI), and a voltage source inverter (VSI), known as pulse-width-modulated (PWM) inverter.

Klug and Mertens (2003) have compared the following converter topologies, from a reliability point of view:

- VSIs with neutral-point clamped inverter (NPC), using high-voltage insulated gate bipolar transistor (IGBTs) or integrated gate commutated thyristors (IGCTs),
- VSIs with a cellular structure of building blocks, using low-voltage IGBTs, and
- LCIs, including a line filter for the reduction of harmonics and power factor correction.

Having compared these topologies for three different power levels: 1.5 MW, 8 MW, and 60 MW, they came to the conclusion that the most simple VSD structures with the fewest components result in the highest reliability. Therefore, an LCI with one redundant thyristor in series is still an appropriate solution in the high MW range. One reason is that it can be run without stopping for regular maintenance to replace defective thyristors. Besides reliability, the selection criteria must also include cost, power quality, efficiency, physical size, complexity, and the footprint of the necessary equipment.

Siebert, et al. (2002), also considered these criteria in comparing multi-Megawatt power electronics but focusing only on the alternating current to direct current (AC to DC) conversion stage, that is, the grid interface of a variable speed drive system. They came to similar conclusions for the reliability because thyristor based systems, such as used in LCIs, have a significantly smaller number of components than systems based on self-commutated devices. They also concluded that all technologies investigated can be configured to meet applicable standard power quality requirements and that thyristor based systems are the most cost effective solution.

Although VSIs can better fulfil the high performance and dynamic requirements of driven loads, LCIs are today the most widespread technology for large drives. These drives are well referenced and have been used in industrial applications for decades despite their drawbacks, such as high total harmonic distortion (THD) on the grid side and high torque ripple on the motor side.

The integer and noninteger harmonics generated by LCIs cause pulsating torque harmonics on the grid side and machine side of the VSD. The presence of an exciting torque component at a torsional natural frequency cannot always be avoided due to the large number of excitations, especially in applications with a wide operating speed range.

Continuously generated harmonic torque excitations could have a critical impact on the torsional behavior of the entire train. However, as far as mechanical resonance excitation is concerned, the most relevant parameter of the electrical excitation source is its frequency (proximity to critical natural frequencies) and the exposure time of excitation, not its magnitude. Therefore, a greater electrical excitation source if not localized close to a mechanical resonant frequency will have less impact on the shaft than a smaller excitation localized at or near that resonant frequency. This explains why torsional issues are also reported in applications where the electrical drive system is based on VSIs, although VSIs are known to produce significantly less torque ripple than LCIs.

It is therefore mandatory to perform torsional analyses during the design stage of large drives, as specified in API 617 (2002). In multi-unit plants, more sophisticated analyses must be performed, which consider the fully coupled electrical and mechanical systems.

LCI PULSATING TORQUE COMPONENTS

In motors driven by power-converters, pulsating torques of various frequencies are superposed on the air-gap torque. As an example, Figure 2 shows two six-pulse thyristor bridges on the grid side (rectifier) and two on the machine side (inverter). In using secondary transformer windings that are 30 degree phase shifted, the pulse number of the rectifier bridge (m) can be increased to $m = 12$, thus reducing the voltage ripple of the rectifier stage. An increase of the pulse number to $n = 12$ is also achieved for the machine side inverter, by 30 degree phase shifted motor windings.

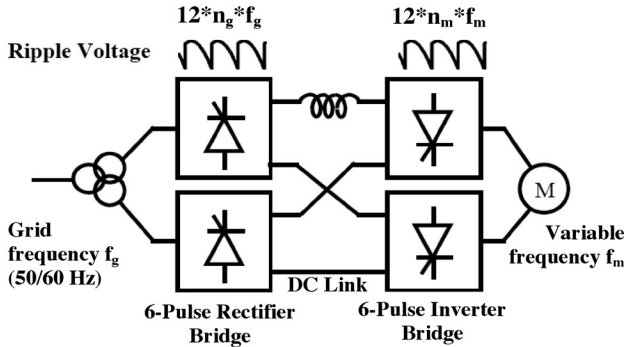


Figure 2. 12/12-Pulse LCI.

The dominant frequencies of the voltage ripple caused by the rectifier and inverter bridges of the 12/12-pulse LCI in Figure 2 are $f_{pulsating} = 12 * f_g$ for the rectifier bridges and $f_{pulsating} = 12 * f_m$ for the inverter bridges, where f_g and f_m are the electrical frequencies on the grid and on the motor side. The harmonic spectrum of the DC link voltage on the grid and machine side also contains multiples of these frequencies.

These voltage ripple waveforms are responsible for integer and noninteger pulsating torque components in the air-gap-torque of the electrical machine. The pulsating torques can be of different types—integer pulsating torques and noninteger pulsating torques.

The pulsating torque caused by an LCI is dominated by integer pulsating torque components, e.g., at $12 * f_g$ and $12 * f_m$. Assuming an electrical frequency of $f = 50$ Hz, the integer pulsating torque components are at 600 Hz and higher. This is typically not an issue for the mechanical system. The noninteger pulsating torques are typically much smaller than the integer torque components. They are generated as interharmonics between the grid side and machine side voltages. Their frequency can be calculated with Equation (1):

$$f_{pulsating} = |n_g \cdot m \cdot f_g \pm n_m \cdot n \cdot f_m| \quad n_m = 1,2,3... \quad n_g = 1,2,3... \quad (1)$$

where:

n, m = Pulse numbers on machine/grid side bridge, $n = m = 12$ in Figure 2

f_g = Electrical frequency on the grid side (50 or 60 Hz)

f_m = Electrical frequency of machine, $= (\text{rpm}/60) * p$ where p is the number of motor pole pairs, typically $p = 1$ or $p = 2$

This set of noninteger pulsating torques is typically most critical in large drives; it covers a large frequency band for harmonic production close to the nominal speed. The effect can be identified in the Campbell diagram, which is a plot of rotational speed dependent pulsating torque frequencies, as given by Equation (1), and torsional natural frequencies of the train.

The Campbell diagram enables one to identify critical operating speeds. The Campbell diagram shown in Figures 3 and 4 belongs to a unit with a nominal speed of 1500 rpm. Potential critical operation speeds are at the crossings of electrical pulsating torque lines and natural mechanical frequencies (horizontal red lines in Figures 3 and 4), and are dependent on the amplitude of the pulsating torque components and on the mechanical damping of the drive train at that torsional natural frequency. For example, if the operational speed is varied by ± 5 percent from the nominal speed, two potential critical operating speeds can be identified in Figures 3 and 4 because of two crossings of line $|12f_g - 12f_m|$ with the first torsional natural frequency (Mode 1) at 20 Hz.

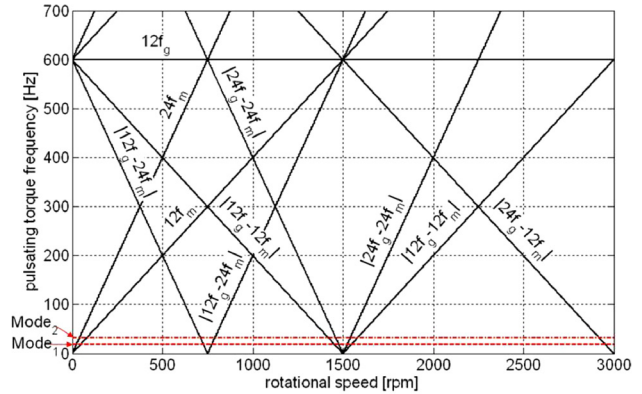


Figure 3. Campbell Diagram of a Compression Train Driven by a 12/12-Pulse LCI (Nominal speed: 1500 rpm).

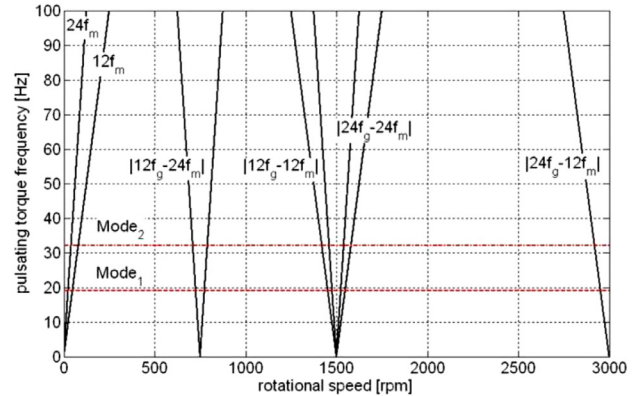


Figure 4. Zoomed Plot of a Campbell Diagram in Figure 3 in the Range 1 to 100 Hz.

It is important to know that the amplitudes of noninteger pulsating torques are typically low in the nominal speed range of a compression train, e.g., less than 1 percent of the nominal torque, as also reported by Simond, et al. (2005). This low level of

electrical excitation at a critical frequency of the mechanical system has also been found by air gap torque measurements during the tests performed with a 30 MW compression train that will be described in more detail in a subsequent section of this paper.

Having noted that in many cases electrical (air-gap) torque components with amplitudes lower than 1 percent of the nominal air-gap torque can cause relevant torsional excitations, the dynamic behavior of the coupled electrical and mechanical system needs to be investigated in more detail. For this purpose, reduced order models for relevant drive train designs are derived in the next section, and recommendations are given for modal damping parameters of models representing synchronous motor driven turbomachines.

MECHANICAL EFFECTS OF PULSATING TORQUES

The first step in a torsional analysis is to generate a lumped parameter model of the mechanical system, as described in more detail by Ong (1999). The differential equation belonging to the reduced order model of two rotating masses (Figure 5) is described by Equation (2) and obtained by applying Newton's second law to a two-mass rotating system with respective inertias J_1 and J_2 and a torsional stiffness K_{12} . θ_1 and θ_2 are the torsion angles.

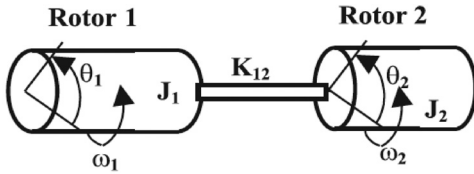


Figure 5. Reduced Order Model of Two Rotating Masses.

Assuming that an external torque of magnitude T_a is applied, and the same frequency as the natural frequency (ω_{nat}) of the mechanical shaft, the torsion angles will oscillate according to Equation (3).

$$\begin{cases} J_1 \frac{d^2 \theta_1}{dt^2} = K_{12}(\theta_2 - \theta_1) \\ J_2 \frac{d^2 \theta_2}{dt^2} = K_{12}(\theta_1 - \theta_2) + T_a \cos(\omega_{nat} t) \end{cases} \quad \text{with } \omega_{nat}^2 = K_{12} \frac{J_1 + J_2}{J_1 J_2} \quad (2)$$

$$\begin{cases} \theta_1(t) = \lambda_1 (t \sin(\omega_{nat} t) + \cos(\omega_{nat} t)) \\ \theta_2(t) = \lambda_2 \left(\frac{J_1}{J_2} t \sin(\omega_{nat} t) - \cos(\omega_{nat} t) \right) \end{cases} \quad \lambda_1 = \frac{T_a}{2(J_1 + J_2)\omega_{nat}} \quad (3)$$

Equation (3) shows that if the externally applied torque has the same frequency as the mechanical resonance frequency of the mechanical system, the torsion angles will increase linearly over time if the mechanical system has no torsional damping. A detailed modeling approach for more complex mechanical systems is described by Song, et al. (2008). A generalized multimass system is shown Figure 6. The differential equation of the system is given by:

$$\mathbf{J} \frac{d^2 \theta}{dt^2} + \mathbf{D} \frac{d\theta}{dt} + \mathbf{K} \theta = \mathbf{T}_{ext} \quad (4)$$

where:

$$\begin{cases} i = 2, 3, \dots, n-1 \\ \mathbf{K}_{1,1} = k_{12} \\ \mathbf{K}_{i,i} = k_{(i-1)i} + k_{i(i+1)} \\ \mathbf{K}_{i,i+1} = \mathbf{K}_{i+1,i} = k_{(i+1)i} = -k_{i(i+1)} \\ \mathbf{K}_{n,n} = k_{(n-1)n} \end{cases}$$

$$\begin{cases} i = 2, 3, \dots, n-1 \\ \mathbf{D}_{i,i} = d_{12} + d_{i0} \\ \mathbf{D}_{i,i} = d_{(i-1)i} + d_{i(i+1)} + d_{i0} \\ \mathbf{D}_{i,i+1} = \mathbf{D}_{i+1,i} = d_{(i+1)i} = -d_{i(i+1)} \\ \mathbf{D}_{n,n} = d_{(n-1)n} + d_{n0} \end{cases}$$

$$\mathbf{J} = \begin{bmatrix} J_1 & \dots & 0 \\ \dots & \dots & 0 \\ 0 & \dots & J_n \end{bmatrix} \quad \mathbf{T}_{ext} = \begin{bmatrix} T_1 \\ \dots \\ T_n \end{bmatrix}$$

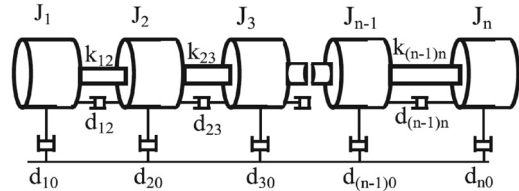


Figure 6. Generalized Representation of a Rotor Shaft System.

The characteristic equation of the system is:

$$[\mathbf{J}^{-1} \mathbf{K} - \lambda \mathbf{I}] = 0, \quad (5)$$

where \mathbf{I} is the identity matrix. The shaft torsional natural frequencies $\omega_{nat,j}$ can be calculated as follows, taking into account the roots λ_j of the characteristic equations:

$$\omega_{nat,j} = \sqrt{\lambda_j}, \quad j = 1 \dots n-1 \quad (6)$$

For an n -mass system, there are $n-1$ eigen frequencies.

Modal damping must be applied to the model, in order to limit the response at resonance to finite values. The modal damping ratio ζ is expressed as a percent of the value for a critically damped system. A critically damped system converges to zero faster than any other without oscillation ($\zeta = 100$ percent). According to Vance (1988), a conservative value of torsional damping for a typical geared turbomachine consisting of a motor, gearbox, and compressor is between $\zeta = 1.5$ percent and $\zeta = 2$ percent.

The modal damping of ungeared systems is typically even lower than that of geared systems. A generic modal damping ratio $\zeta = 1.25$ percent has been found to be a conservative assumption for ungeared systems, in the absence of actual test data. This corresponds to an amplification factor Q of 40.

The relationship between the damping ratio ζ and the amplification factor Q is given by Equation (7).

$$Q = \frac{1}{2\zeta} \quad (7)$$

The modal damping can also be expressed by the logarithmic decrement Λ . For an exponentially decaying oscillation as shown in Figure 7, Λ can be determined by comparing the amplitudes of two subsequent peaks $q(t_0)$ and $q(t_0 + nT)$, as defined in Equation (8).

$$\Lambda = \frac{1}{n} \ln \left| \frac{q(t_0)}{q(t_0 + nT)} \right| \quad (8)$$

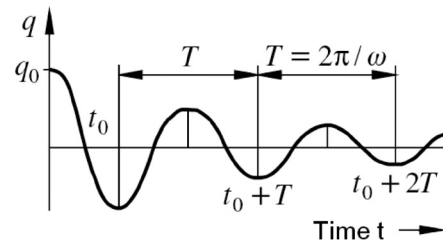


Figure 7. Explanation of the Logarithmic Decrement Λ Used in Equation 8.

Λ is a useful quantity in practical applications because the modal damping can be determined from the measured torsional response of the mechanical system after a step load is applied. For electric motor-driven turbomachinery such measurement results can be achieved after trip events of the electric motor.

Another way of expressing modal damping values is to indicate the real part σ of the eigenvalue of a mode. In weakly damped systems, the relationship between σ , Λ , and ζ is given by Equation (9):

$$\sigma = \zeta \cdot \omega_{nat,j} = \frac{\omega_{nat,j}}{2\pi} \Lambda \quad (9)$$

σ , ξ , or Λ can also be calculated by determining Q in the frequency domain. This is demonstrated in Figure 8, showing the harmonic analysis of a torsional oscillation that was measured in a 144 MVA flywheel generator application by Sihler (2006). In this example, the rotor shaft system had a first natural frequency of 23.82 Hz. Q can be determined from the forced response of the mechanical system, after exciting the generator rotor with small amplitude air-gap torque harmonics that contained frequency components close to 23.8 Hz. In this test Q was calculated from the shape of the torque peak in the harmonic analysis, by Equation (10):

$$Q = \frac{f_0}{f_2 - f_1} = \frac{23.82\text{Hz}}{23.88\text{Hz} - 23.76\text{Hz}} = 198.5 \quad (10)$$

where:

- f_0 = First natural torsional frequency of train
- $f_{1,2}$ = Frequencies at the two points where the torque amplitude q in Figure 8 has decreased from its maximum to a value of $\hat{q}_{\max}/\sqrt{2}$

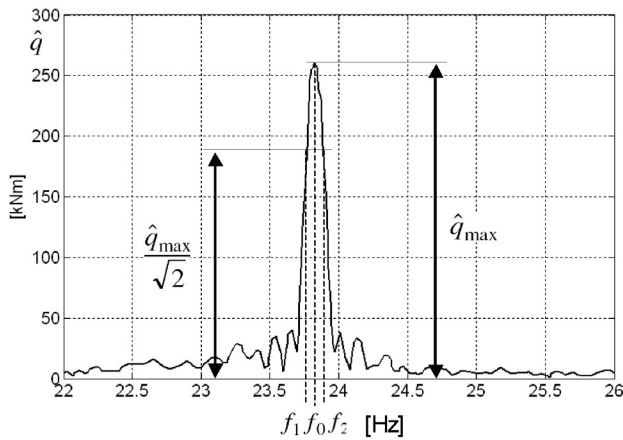


Figure 8. Harmonic Analysis of a Torsional Oscillation: Determination of Amplification Factor Q in Measuring f_0 , f_1 , and f_2 (1 kNm = 738 lbf ft).

In this application, an amplification factor $Q \approx 200$ was determined. Although this high Q factor was not measured in an oil and gas industry application, this measurement result seems relevant because it shows that amplification factors (Q) higher than those given by Vance (1988) can be experienced when directly driving high-power trains with synchronous machines.

Such low damping is in line with the values assumed for subsynchronous torsional modes of oscillation of large turbine generators for utility applications. The authors' company has worked on many such projects since the early 1970s, and measured values for inherent mechanical damping range from lows of $\sigma = 0.02 \text{ s}^{-1}$ at minimum power to $\sigma = 0.4 \text{ s}^{-1}$ at maximum power (these translate to Q above 4000 at low load to near 200 for full load). When damping is not known, the practice is generally to assume a conservative range of $\sigma = 0.02 \text{ s}^{-1}$ ($Q=4000$) at no load and $\sigma = 0.2 \text{ s}^{-1}$ ($Q = 400$) at full load. Selected references are included for these utility-class machines: Walker, et al. (1978); Bowler, et al. (1978); Piwko, et al. (1988).

It is important to understand that the damping will be a function of load level in the compressors/turbines on the shaft, and also a function of the torsional mode shape. For torsional modes where the motor is moving much more than the turbine/compressor sections, the damping will be much lower.

Table 1 summarizes the amplification factors reported in literature for synchronous machines driving turbomachinery and for power generation applications, together with the rated power of the synchronous machines.

Table 1. Summary of Amplification Factors Q Reported in Literature for High Power Trains Driven by Synchronous Machines.

Application	Typical Nominal Power	Torsional Nat. Freq. of Interest	Q
G geared turbomachine	<50 MW	< 200 Hz	25-33
Ung geared turbomachine	<50 MW	< 200 Hz	40
Flywheel generator	150 MW	20-30 Hz	200
Power generation (utility steam turbines)	<1000 MW	8-150 Hz	400 (full load) to 4000 (at light load)

As can be seen from Table 1, generic values for the torsional modal damping must be applied with high care, especially in new applications with synchronous motor-driven turbomachinery and high power ratings. If the actual Q value is not known, conservative values derived from similar designs should be used until measurement results become available.

MEASUREMENT OF TORSIONAL VIBRATIONS

Standard equipment used for analyzing lateral vibrations, such as accelerometers and proximity probes, are not able to measure torsional vibrations. Depending on the shape of the torsional mode and the stiffness of the motor coupling, even high-resolution motor speed measurements may not be able to accurately measure such vibrations. In string tests, torsional vibration measurements are typically based on measuring the shaft torque, e.g., by a full-bridge strain gauge system with telemetry. If the shaft torque has to be monitored over long time periods or if the torque signal is used in a control system, long-term stable measurement methods have to be applied.

Examples for suitable sensing systems are continuous duty (CD) torque-meters for permanent installation, which are offered by a variety of vendors. The most widespread CD sensing technology is based on measuring the twist over a coupling spool, and there are more than 800 installations worldwide using this approach with many millions of operating hours accumulated.

To achieve absolute accuracy of the torque measurement in the order of 1 percent full scale, such torque-meters must be integrated into the mechanical system design, typically during the design stage. Therefore it can be costly to apply this type of torquemeter as a retrofit.

However, for torsional mode damping applications, an absolute accuracy of 1 percent full scale is not needed. The most important measured signals in this type of feedback control system are the frequency and phase of a measured oscillation. Therefore, alternative noncontact sensing methods with high long-term stability may be more attractive. As an example, toothed-wheel based monitoring systems have a long history of measuring torsional vibrations continuously on utility-class generating machines.

Proper transduction of the pulses from the sensors, plus knowledge of the torsional mode shapes, are adequate for detecting torsional vibrations sufficient for both protection and damping, as reported by Piwko, et al. (1996). This type of sensing and monitoring system has been used in several dozens of applications with synchronous generators over the last 30 years.

Recently, in another power system application, a magnetostrictive torque sensing system, as described by Wirsén and Kulig (2007), was installed to monitor the shaft torque at the couplings of two large flywheel generators. The torque measurements are used for a torsional mode damping control of the two generators, described in more detail by Sihler and Miri (2005). The frequent torsional interactions with thyristor converter based loads and the high amplification factors Q of the flywheel generator trains ($Q = 200$, refer to Table 1) were the reasons for applying torsional mode damping to each generator. The absolute accuracy of the torque

sensors in this application is only in the lower percent range. However, reliable and stable damping has been achieved based on the magnetostrictive measurement input, see Käsemann, et al. (2009). This type of torsional vibration sensing is well suited for retrofit applications because it does not require attachment to the rotating shaft or modification of the existing train.

INTEGRATED TORSIONAL MODE DAMPING DESIGN FOR LCI-DRIVEN TURBOMACHINERY

Integrated torsional mode damping (ITMD) is an electro-mechanical damping method integrated with the electrical drive control. ITMD was developed to make synchronous motor-driven turbomachinery less sensitive to critical motor-driven torque harmonics and patented by Sihler and Song (2006). Figure 9 shows a typical VSD drive train arrangement with an externally applied ITMD control. As discussed in the previous section, the pulsating torque components introduced through the air-gap-torque can excite a torsional natural frequency of the mechanical system. Assuming operation at a critical speed, the resulting torsional oscillation can be measured in the driven load. The resulting amplitude of the dynamic torque component depends on the mechanical damping of the drive train.

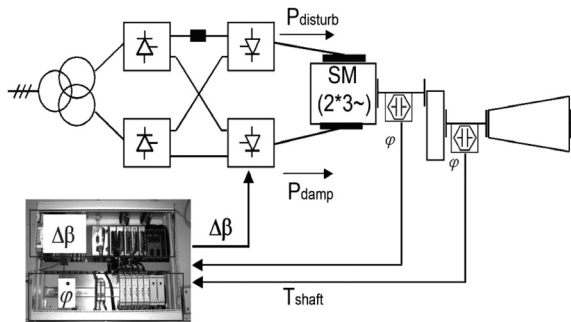


Figure 9. LCI Driven Compressor with External ITMD Control System (SM: Synchronous motor, ϕ : Measured torque at low speed and high speed shaft, $P_{disturb}$: Disturbance power caused by LCI torque ripple, P_{damp} : Damping power caused by ITMD).

The location of the sensors measuring dynamic torque components in the mechanical system has to be chosen based on the calculated eigenvector (mode shape). The measured dynamic reaction of the mechanical system is fed into an embedded controller, processed, and sent to the machine-side firing angle of the VSD machine converter bridge (β -angle).

The block diagram of an LCI control system is shown in Figure 10. The line converter, controlled by means of the firing angle α , executes the closed loop control functions that are most relevant for the end user, such as the torque (if available) and speed control of the variable speed drive. The machine converter has a feed forward control, beta (β)-control, that is typically designed to achieve an optimum power factor on the machine side. The end user has typically no access to the β -control.

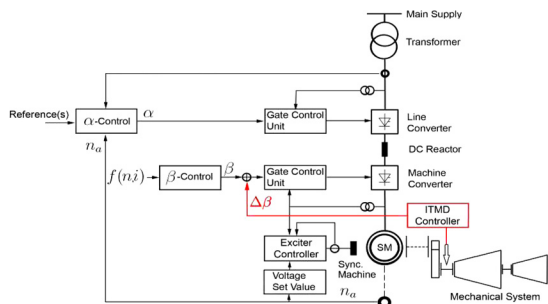


Figure 10. Block Diagram of LCI Drive Control System with Integrated ITMD Controller.

Figure 10 also shows that an ITMD control can be achieved by adding a small signal modulation ($\Delta\beta$) to the output signal of the β -control. The interface for the modulation signal must be provided at the output of the β -control block because the β -control is a control system that is typically not designed for handling signals with a bandwidth of tens of Hz.

The β -angle modulation signal ($\Delta\beta$) has the same effect as increasing the mechanical damping, because it generates an additional air-gap torque with a frequency component that is identical to a torsional natural frequency of the mechanical system but lagging an existing mechanical torque oscillation by 90 degrees, as shown in Figure 11.

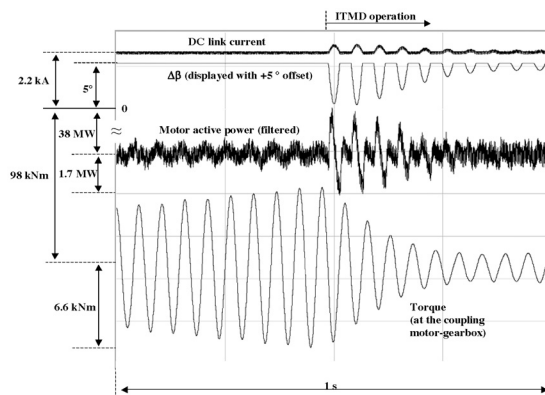


Figure 11. Simulated Effect of Torsional Mode Damping for a 50 MW Natural Gas Compression Train with a Design as Shown in Figure 10 (but the torque measured at the coupling motor-gearbox, $1\text{kNm} = 738\text{ lbf ft}$).

Figure 11 shows the results of a coupled electro-mechanical simulation where a synchronous motor-driven compressor is operated at a torsional critical speed. The embedded damping controller is disabled during the first 0.5 seconds of the plot. At this time, the dynamic torque component oscillating at the first torsional natural frequency grows. After enabling the embedded controller (“ITMD operation”), the dynamic torque component decreases. The remaining dynamic torque component depends on the closed loop gain of the damping control.

The objective of the damping control is not to totally suppress a torsional reaction of the mechanical system but to keep the torsional stress at a critical speed within safe operating limits. Only for illustration purposes, it was assumed that the damping control causes a β -angle modulation of 5 degrees in Figure 11. Such high $\Delta\beta$ values do not have to be applied in industrial applications.

Figure 12 shows dynamic torque measured at the motor coupling during a string test where an ITMD was applied to a natural gas compression train with a nominal power of about 50 Megawatts. Since a shaft torque measurement based on strain gauges with telemetry was readily available, the input signal for the ITMD control was derived from this torque measurement. The measured data show that a small modulation of the inverter β -angle (1.5 degree in this example) has a strong effect on the mechanical system.

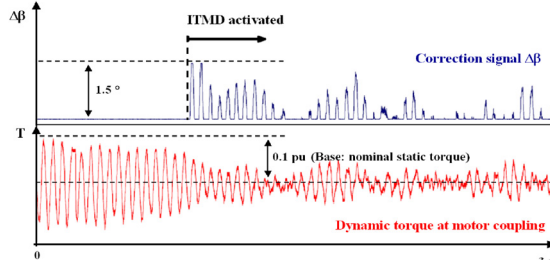


Figure 12. Measured Effect of Torsional Mode Damping Control (ITMD) Tested During String Tests with a 50 MW Natural Gas Compression System.

The applied β -angle modulation of 1.5 degree corresponds to an active power modulation of less than 0.5 percent of the nominal power. The effect on the machine side power factor is negligible (less than 1 percent), considering that the $\Delta\beta$ signal oscillates between 0 and 1.5 degree. This results in an average value of 0.75 degree that is subtracted from a static β -angle of typically 150 degrees, and only for the short time of damping with full damping power.

The active damping power, acting in addition to the natural torsional damping of the train, was sufficient to reduce the torsional oscillations at the first natural frequency of the 50 Megawatt train by more than a factor of two. The amount of damping power applied can safely be limited to the value that corresponds to the maximum β -angle modulation, e.g., to 2 or 3 degrees.

Thus, the ITMD control unit shown in Figure 9 can be designed as an external, retrofit extension for a given LCI control system. Since ITMD control has negligible impact on the electrical system, it does not require changes to the drive system design, only an additional interface to the machine side (inverter) β -control.

Integrated torsional mode damping was specially developed for LCIs, being the most widespread technology for large drives and having an excellent reliability record. A disadvantage is the limited bandwidth of their control system because of design constraints of thyristor-based converters. But the objective of ITMD control is not to eliminate critical air-gap torque harmonics that would require a response of the drive system in real-time (maximum delay times in the range of tens of microseconds) but to keep the resulting torsional vibrations within safe limits.

ITMD control is a “mechatronic” approach where one or more sensors in the mechanical system are utilized to create damping torque components for torsional oscillations in the rotor shaft system, by means of the electric drive and motor. These damping torque components are represented by T_{ext} in Equation (11)—refer to Equation (4) for an explanation of the other equation elements:

$$J \frac{d^2\theta}{dt^2} + D \frac{d\theta}{dt} + K\theta = T_{ext} \quad (11)$$

In generating the electrical (air-gap) torque using a feedback loop as shown in Figure 9, pulsating T_{ext} components acting through the electrical motor can have the same effect as increased damping for single torsional modes, represented by vector $D \cdot d\theta/dt$ in this equation. With this approach, not all torsional modes of a complex drive train can be damped. But it is obvious that this method can be applied to all torsional vibrations that are excited by pulsating air-gap torque components caused by an electric drive system. Therefore, the ITMD method is not restricted to being used with LCIs. It can also be applied to VSIs to eliminate risks with low order torque harmonics when driving large drive trains.

A significant advantage of this active damping approach is that it does not require real-time behavior of the electrical drive control, as explained by Figure 13. In the simulation it was assumed that a “disturbance power” (blue curve), i. e., an air-gap torque harmonic with a critical torsional frequency, excites a torsional vibration (upper curve) in a synchronous motor driven train with low natural damping ($Q = 80$), between $t = 2.5$ seconds and $t = 3.4$ seconds. At $t = 3.0$ seconds, the ITMD control is activated. The correction signal applied causes additional damping power (green curve in Figure 13) with a sine-wave shape.

With an approach that tries to compensate for or eliminates the disturbing air-gap torque, it is necessary to react immediately to any disturbance causing torsional issues. But with a damping approach exemplified by Equation (11), dynamic torque components can be limited to desired values, without fast control actions, thus enabling this solution to be implemented with the given drive control system.

The control system of an LCI, being a thyristor-based converter, cannot be designed to achieve real-time behavior, which would be needed for cancelling critical air-gap torque harmonics. The difference in the effect of a torsional mode damping approach and

an approach that tries to compensate for the electrical excitation source is shown in the red curve of Figure 13. The ITMD method achieves a strong damping effect without trying to eliminate critical frequencies in the air-gap torque.

The red curve in Figure 13 (T_{air}) results from the electrical torques caused by the disturbance power p_{dist} and damping power p_{damp} (refer also to Figure 9). If a fast Fourier transform (FFT) were performed on the air-gap torque before and after applying ITMD, that is at $t < 3.0$ seconds and $t > 3.0$ seconds respectively, about the same amount of critical frequency components would be measured in the air-gap torque T_{air} . This differs from an “active noise cancellation” approach.

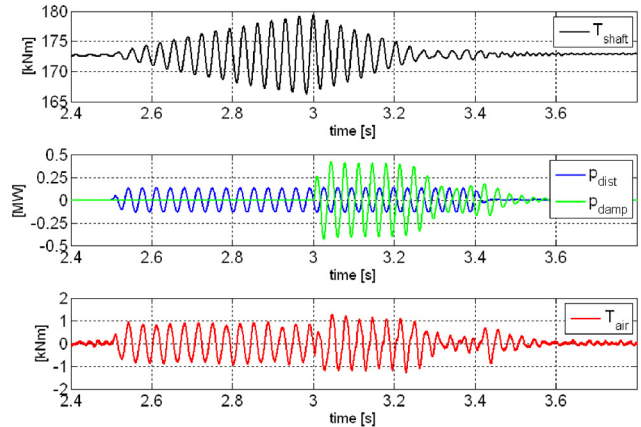


Figure 13. Simulated Effect of Torsional Mode Damping Applied to an LCI Driven 30 MW Compression Train (1kNm = 738 lbf ft).

The integrated torsional mode damping method has several unique features that are important for high power applications:

- Demonstrated high gain margin resulting in a very robust design
- The applied damping power can be limited in a failsafe manner by limiting the β -angle modulation to small values.
- ITMD can be applied without changes to the installed electrical and mechanical system.

This section of the paper has demonstrated that ITMD has the same effect as increased natural damping of the mechanical train but with the advantage that the damping is electronically adjustable. Another advantage of this damping method is the robustness against small variations in the torsional natural frequency because it is based on continuous feedback from a torque meter or a torsional vibration measurement.

ITMD CONTROL FOR EXTENDED VARIABLE SPEED OPERATION OF COMPRESSORS

ITMD control makes the drive train more robust against electrical disturbances. This is beneficial in cases where a coincidence of electrical drive harmonics and natural torsional frequencies of the mechanical system is unavoidable, e.g., due to an extended variable speed range of the compressor such as for process requirements. For instance, referring to Figures 3 and 4, in an application where the nominal speed of the compressor is 1500 rpm and the operational speed can be anywhere between 90 percent and 105 percent of the nominal speed, a crossing of critical speeds may occur. It may be required that the rate of change of speed is low while crossing the critical speed or that the compressor is operated at a critical speed.

An LCI drive applied in a project with such requirements had a nominal power rating of about 30 Megawatts and was designed to generate air-gap torque harmonics at critical speeds with a

maximum amplitude of less than 1 percent of the nominal torque. The fulfilment of this electrical requirement was confirmed during string test measurements.

As additional protection during the string test, an ITMD control unit was installed. The torque measurement used for ITMD control was based on an existing strain gauge measurement system with telemetry. Test results are shown in Figures 14 to 19. Figures 14 and 15 show the crossing of a critical speed with a ramp rate of 2.5 rpm/s. The test shown in Figure 14 was performed with ITMD control deactivated.

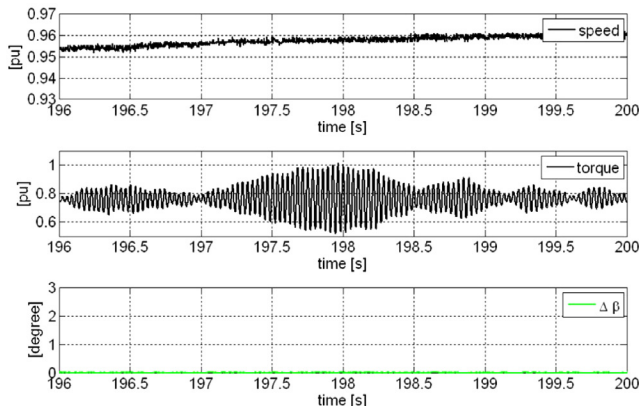


Figure 14. Measured Torsional Reaction of 30 MW Gas Compression Train While Running Through a Critical Speed Without ITMD Control (Ramp rate: 2.5 rpm/s) Speed and Torque Expressed in PU Based on Nominal Speed and Torque.

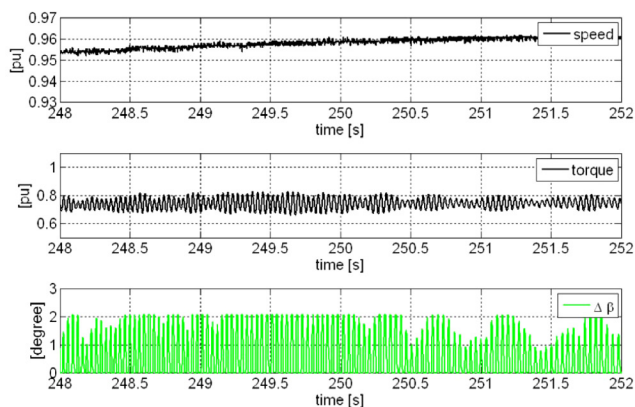


Figure 15. Measured Torsional Reaction of 30 MW Gas Compression Train While Running Through a Critical Speed with ITMD Control (Ramp rate: 2.5 rpm/s).

Figure 15 shows a repetition of this test run with torsional mode damping control. The $\Delta\beta$ -angle modulation (correction signal for LCI inverter control) was limited to 2 degrees during the tests. This limitation corresponds to a damping power of less than 1 percent of the nominal power of the drive system. Despite this limitation, the ITMD control was able to suppress the torsional resonance when crossing a critical speed.

The same experiment was repeated with negative ramp rates (Figure 16 and 17), different speed rates, at other critical speeds, and with different settings of control parameters. The results were consistent in that ITMD control provided sufficient additional damping to operate the rotating system at any speed in the desired operating range. The additional damping power provided by ITMD was always limited to less than 1 percent of the nominal power of the system.

The string tests performed with a 30 MW compression train with ITMD control also included fault analyses for the damping control. For instance, as shown in Figures 18 and 19, the authors investigated what happens when the train is operated at a critical speed, and the ITMD control is switched off for a few seconds and then back on.

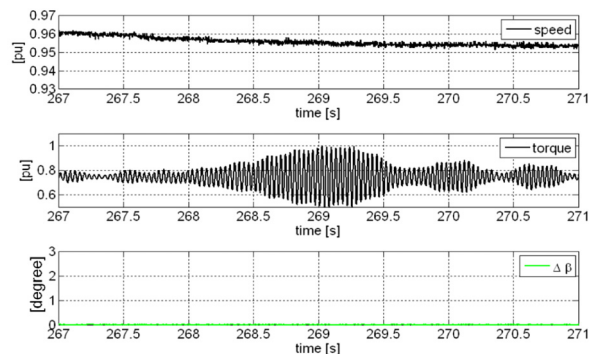


Figure 16. Measured Torsional Reaction of 30 MW Gas Compression Train While Running Through a Critical Speed Without ITMD Control (Ramp rate: -2.5 rpm/s).

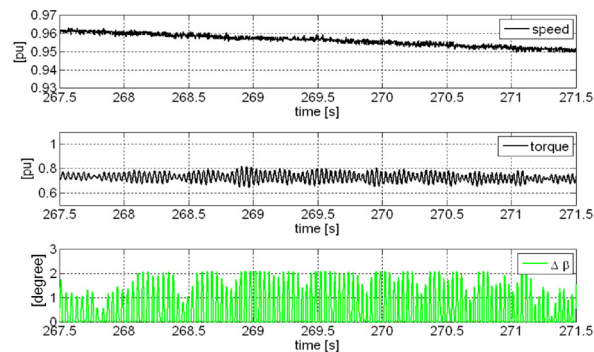


Figure 17. Measured Torsional Reaction of 30 MW Gas Compression Train While Running Through a Critical Speed With ITMD Control (Ramp rate: -2.5 rpm/s).

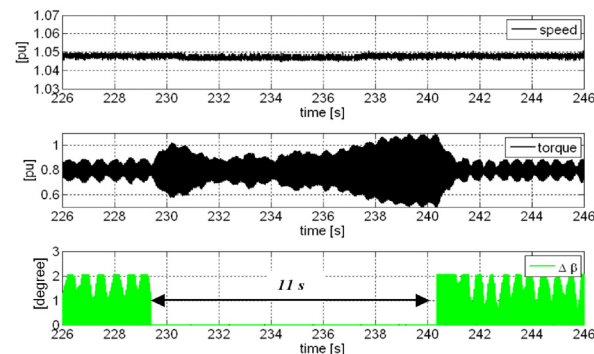


Figure 18. Measured Torsional Dynamics of a 30 MW Compression Train Operated at a Critical Speed with ITMD Control Deactivated for 11 s.

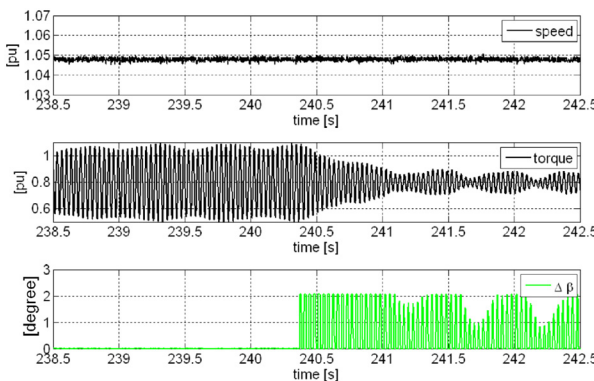


Figure 19. Measured Torsional Dynamics of a 30 MW Compression Train Operated at a Critical Speed—Activation of ITMD Control at 240.3 s (Zoom of Figure 18).

In this experiment the speed reference was kept at a constant value. However it can be seen in Figure 18 that unwanted speed deviations occurred during the test. The exact actual speed strongly influences the dynamic torque amplitude during resonance excitation, but only during the 11 seconds for which the ITMD control was turned off. When the ITMD control was reactivated, at $t = 240.3$ seconds, less than one second was needed to damp the dynamic torque components down to values that are well within the alternating torque limits of the shaft.

Also visible in Figure 19 is that the correction signal was driven to saturation during this test, resulting in a square wave shape of the correction pulses $\Delta\beta$ instead of the positive sine wave pulses applied previously (refer to Figure 12). The square wave pulses do not cause negative effects because their fundamental frequency corresponds to the natural torsional frequency to be damped. This can be seen when performing a Fourier transformation of the $\Delta\beta$ signal. The reason for the saturation was the high dynamic torque amplitudes reached while the ITMD control was switched off. The test with saturated correction signal was part of the sensitivity analysis and demonstrates that reliable damping is also achieved in cases where the correction pulses are distorted.

SUMMARY OF THE ITMD STRING TEST RESULTS AND OUTLOOK

The tests performed with an electrically driven 30 Megawatt compression train demonstrated that ITMD control is a very effective way of damping torsional resonances. In cases where the drive system generates air gap torque harmonics with amplitudes higher than 1 percent at a critical frequency, it would be possible to generate more damping power through the torsional mode damping control system, as demonstrated in Figure 11. However, based on experience, it is sufficient to provide damping power that is significantly lower than the maximum disturbance power because the ITMD damping is added to the inherent natural damping of the mechanical system. For industrial applications, a damping power of typically 1 percent of the rated system power seems sufficient to effectively damp torsional vibrations.

Example Showing Damping of Several Modes

Torsional mode damping control is not limited to damping only single torsional modes. In more complex drive train arrangements, several modes can be damped simultaneously if needed, by a more sophisticated design of the damping control system. An example of such a system is shown in Figure 20.

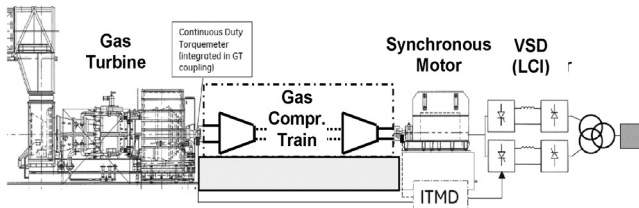


Figure 20. Large Electrically Driven Compression Train with Damping Control for Up to Three Torsional Modes.

A torsional mode damping control for the first three torsional modes of this mechanical arrangement was designed and investigated using numerical simulations. The first two torsional modes were measured by an existing continuous duty torquemeter, integrated into the gas turbine coupling. For measuring the third torsional mode, an additional torquemeter was installed at the motor coupling.

Illustrative simulation results (assuming that two of the torsional modes are being excited) are shown in Figures 21 and 22. These two figures show time histories of the simulated shaft torque at different locations of the compression train of Figure 20: T_{GT-C1} is the torque at the gas turbine coupling, T_{C3-EM} can be measured at the

motor coupling, T_{C1-C2} and T_{C2-C3} represent shaft torque between compressor stages. It is unlikely that two modes would be excited simultaneously, but this case was investigated to ensure that several modes can be damped without nuisance interactions. Additional simulations were performed to ensure that satisfactory torsional mode damping can be achieved in cases where either single modes or up to three modes are excited by motor air-gap torque harmonics.

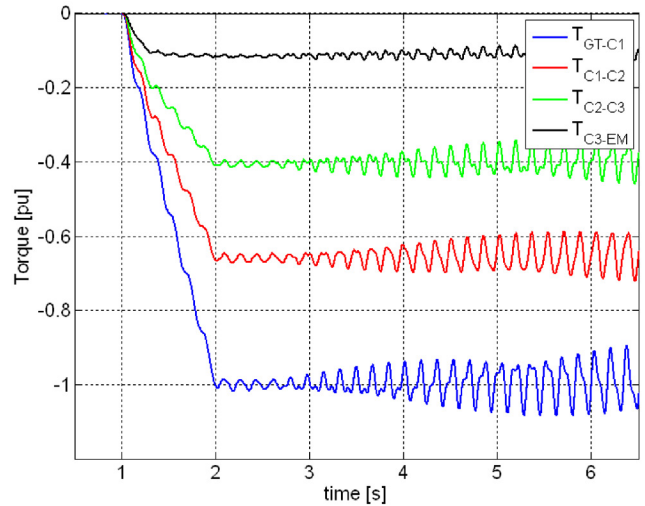


Figure 21. Simulated Mechanical Shaft Torques for Figure 20 Compression Train (Assumed: first two torsional modes excited by small air-gap torque ripple at $t > 2.5$ s, T_{GT-C1} : Torque at gas turbine coupling, T_{C3-EM} : Torque at the motor coupling, T_{C1-C2} and T_{C2-C3} : Torque between compressor stages) Torque is Expressed in PU Based on Nominal Torque.

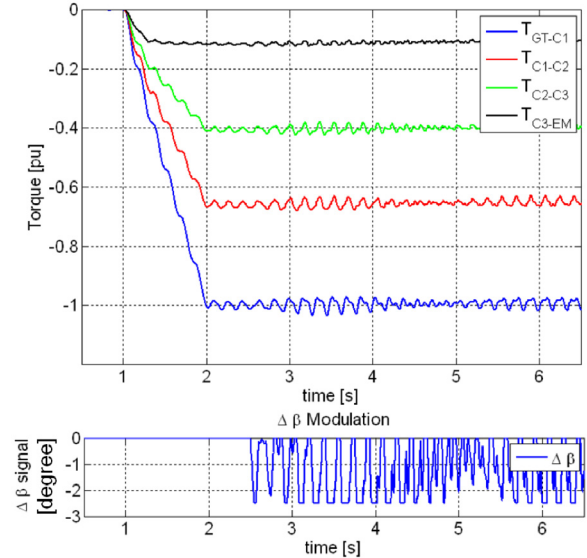


Figure 22. Simulated Torsional Reaction of ITMD Controlled Compression System (Same mechanical system and load case as in Figure 21). The Correction Signal $\Delta\beta$ (Lowest curve) Is Composed of Two Main Frequency Components.

Example with Island Power System Topology

Integrated damping control can be applied with driven loads, on the motor side of the drive as shown in this paper, but it can also be used for generators on the grid side of a large variable speed drive. Some oil and gas production sites employ island power systems, e.g., on offshore platforms. An example for a simple topology is shown in Figure 1c. The risk of operational problems increases with

increasing size and percentage of the converter loads, i.e., with increasing converter power relative to the short circuit power level of the grid.

To mitigate the risk of torsional issues with an increasing percentage of converter loads in a weak power system, one or more of the LCI control systems can be equipped with a torsional mode damping control, acting on the rectifier bridge of the variable speed drive system, as described in Sihler and Song (2006). A benefit of torsional mode damping in generator applications is that it can be applied in cases where the source of excitation is not exactly known (e.g., a small excitation source) because its effect is to make the generator train less sensitive to critical air-gap torque harmonics.

CONCLUSIONS

Variable speed electric drives enable increased operational flexibility and energy efficiency. Issues with variable speed driven systems may arise from the generation of air-gap torque ripple components due to electrical harmonics and the fact that synchronous motor-driven turbomachinery can have inherently low mechanical damping values. Therefore, executing a traditional torsional analysis, as described in API 617 (2002), is an essential step during the design stage. In addition, a fully coupled electrical and mechanical analysis may be required to predict the dynamic behavior of the train under all operating conditions.

The accuracy of numerical analyses performed on new equipment is limited by the input parameters used in the simulation. Examples are:

- Limitations in the accuracy of calculated mechanical damping values before actual test data are available,
- Pulsating torque components caused by the drive system during the electrical commissioning or as a consequence of malfunctions,
- Interharmonic interactions caused by other VSD loads connected to the same power system, and
- Dynamic torque components caused by aerodynamic effects in compressors or turbines.

The sensitivity of electrically-driven compression trains to harmonic torque ripple components and other disturbances can be decreased by adding a torsional mode damping controller to the electrical drive system. Integrated torsional mode damping is based on input from sensors in the mechanical system, to ensure reliable operation and optimum performance for high power trains with complex rotordynamics. The damping power caused by an ITMD control is typically limited to a very low value, e.g., less than 1 percent of the nominal power of the motor. Therefore, this system can be used as a retrofit for existing drive system designs, e.g., in cases where torsional issues have already occurred, or as an integrated solution for string tests with new equipment as risk mitigation where torsional issues cannot be totally excluded.

NOMENCLATURE

LCI	= Load commutated inverter
ITMD	= Integrated torsional mode damping
LNG	= Liquefied natural gas
GT	= Gas turbine
ST	= Steam turbine
M	= Motor
G	= Generator
THD	= Total harmonic distortion
VSD	= Variable speed drive
VSI	= Voltage source inverter
P_m, P_g	= Pulse numbers on machine/grid side bridge
f_m, f_g	= Electrical frequency on the machine/grid side
J_1, J_2	= Moments of inertia
K_{12}	= Stiffness constant
T	= Torque

θ	= Torsion angle
ω_{nat}	= Natural angular frequency
$f_{pulsating}$	= Frequency of pulsating air-gap torques
ζ	= Damping ratio
Q	= Amplification factor, $Q = 1/(2D)$
Λ	= Logarithmic decrement
CD	= Continuous duty
FFT	= Fast Fourier transformation
β -angle	= Motor side (inverter) firing angle
$\Delta\beta$	= Modulation of inverter firing angle
J	= Matrix of moments of inertia
D	= Damping matrix
K	= Stiffness matrix
φ	= Vector of torsion angles
u	= Vector of externally applied torques
B	= Input matrix for external torques

REFERENCES

- API Standard 617, 2002, "Axial and Centrifugal Compressors and Expander-Compressors for Petroleum, Chemical and Gas Industry Services," Seventh Edition, American Petroleum Institute, Washington, D.C.
- Baccani, R., Zhang, R., Toma, T., Iuretig, A., and Perna, M., 2007, "Electric Systems for High Power Compressor Trains in Oil and Gas Applications—System Design, Validation Approach, and Performance," *Proceedings of the Thirty-Sixth Turbomachinery Symposium*, Turbomachinery Laboratory, Texas A&M University, College Station, Texas, pp. 61-68.
- Bowler, C. E. J., Baker, D. H., Mincer, N. A., and Vandiveer, P. R., 1978, "Operation and Test of the Navajo SSR Protective Equipment," *IEEE Transactions on Power Apparatus and Systems*, PAS-97, July/August, pp. 1030-1035.
- Käsemann, C. P., van Lieshout, L., Huart, M., and Rott, M., 2009, "10 MVA Thyristor Converters for the Active Damping of Generator Shaft Oscillations at ASDEX Upgrade," *Elsevier, Fusion Engineering and Design*, in press, available online at www.sciencedirect.com.
- Klug, R. D. and Mertens, A., 2003, "Reliability of Megawatt Drive Concepts," *ICIT2003*, Maribor, Slovenia, pp. 636-641.
- Ong, C. M., 1999, *Dynamic Simulation of Electric Machinery Using Matlab/Simulink*, Prentice Hall.
- Piwko, R. J., Kankam, M. D., Baker, D. H., Wu, C. T., and Peterson, K. J., 1988, "The Intermountain Power Project Commissioning—Subsynchronous Torsional Interaction Tests," *IEEE Transactions on Power Delivery*, 3, October, pp. 2030-2036.
- Piwko, R. J., Wegner, C. A., Kinney, S. J., and Eden, J. D., 1996, "Subsynchronous Resonance Performance Tests of the Slatt Thyristor-Controlled Series Capacitor," *IEEE Transactions on Power Delivery*, 11, (2), April, pp. 1112-1119.
- Siebert, A., Troedson, A., and Ebner, S., 2002, "AC to DC Power Conversion Now and in the Future," *IEEE Transactions on Industry Applications*, 38, (4), July/August.
- Sihler, C., 2006, "A Novel Torsional Exciter for Modal Vibration Testing of Large Rotating Machinery," *Mechanical Systems and Signal Processing*, Elsevier, 20, pp. 1725-1740.
- Sihler, C. and Miri, A. M., 2005, "A Stabilizer for Oscillating Torques in Synchronous Machines," *IEEE Transactions on Industry Applications*, 41, (3), May/June, pp. 748-755.
- Sihler, C. and Song, J., 2006, "Integrated Torsional Mode Damping System and Method," *International Patent Corporation Treaty*, PCT/US2006/013508, Apr. 2006, US Patent 7,173,399, February 2007.

- Simond, J. J., Sapin, A., Tu Xuan, M., Wetter, R., and Burmeister, P., 2005, "12-Pulse LCI Synchronous Drive for a 20 MW Compressor—Modeling, Simulation and Measurements," IEEE Transactions on Industry Applications, pp. 2302-2308.
- Song, J. Sihler, C., and Nyobe, J. M., 2008, "Modeling of Torsional Resonances for Multi-Megawatt Drives Design," IEEE Industry Applications, Annual Meeting, Edmonton, Canada, October 2008, available online at IEEE Xplore 978-1-4244-2279-1/08.
- Vance, J. M., 1988, *Rotordynamics of Turbomachinery*, Edition 1, John Wiley & Sons.
- Walker, D. N., Bowler, C. E. J., and Baker, D. H., 1978, "Torsional Dynamics of Closely Coupled Turbine-Generators," IEEE Transactions on Power Apparatus and Systems, PAS-97, (4), July/August, pp. 1458-1465.
- Wirsen, A. and Kulig, S., 2007, "A Contact-Less Torque Sensor for Online Monitoring of Torsional Oscillations," Fraunhofer Institute ITWM 2007, available online: http://www.itwm.fhg.de/as/asproducts/torsion/Flyer_Sensor_ITWM_en.pdf.

